

## 6. RADIATION SOURCES AND OPTICS

### 6.1. X-ray sources

BY U. W. ARNDT

#### 6.1.1. Overview

In this chapter we shall discuss the production of the most suitable X-ray beams for data collection from single crystals of macromolecules. This subject covers the generation of X-rays and the conditioning or selection of the X-ray beam that falls on the sample with regard to intensity, cross section, degree of parallelism and spectral composition. The conclusions drawn do not necessarily apply to smaller-unit-cell crystals or to noncrystalline samples.

#### 6.1.2. Generation of X-rays

X-rays are generated by the interaction of charged particles with an electromagnetic field. There are four sources of interest to the crystallographer.

(1) The bombardment of a target by electrons in a vacuum tube produces a continuous ('white') X-ray spectrum, called *Bremsstrahlung*, which is accompanied by a number of discrete spectral lines characteristic of the target material. The most common target material is copper, and the most frequently employed X-ray line is the copper  $K\alpha$  doublet with a mean wavelength of 1.542 Å. X-ray tubes are described in some detail in Chapter 4.2 of *ITC* (1999). We shall consider only the most important points in X-ray tube design here.

(2) Synchrotron radiation is produced by relativistic electrons in orbital motion. This is the subject of Part 8.

(3) The decay of natural or artificial radioisotopes is often accompanied by the emission of X-rays. Radioactive sources are often used for the testing and calibration of X-ray detectors. For our purposes, the most important source is made from  $^{55}\text{Fe}$ , which has a half-life of 2.6 years and produces Mn  $K\alpha$  X-rays with an energy of 5.90 keV.

(4) Ultra-short pulses of X-rays are generated in plasmas produced by the bombardment of targets by high-intensity sub-picosecond laser pulses (*e.g.* Forsyth & Frankel, 1984). In earlier work, the maximum pulse repetition frequency was much less than 1 Hz, but picosecond pulses at more than 1 Hz are now being achieved with  $\mu\text{m}$ -size sources. The time-averaged X-ray intensities from these sources are very low, so their application will probably remain limited to time-resolved studies (Kleffer *et al.*, 1993).

X-rays also arise in the form of channelling radiation resulting from the bombardment of crystals, such as diamonds, by electrons with energies of several MeV from a linear accelerator (Genz *et al.*, 1990) and in the form of transition radiation when multiple-foil targets are bombarded by electrons in the range 100–500 MeV (*e.g.* Piestrup *et al.*, 1991). It will be some time before these new sources can compete with the older methods for routine data collection.

##### 6.1.2.1. Stationary-target X-ray tubes

A section through a permanently evacuated, sealed X-ray tube is shown in Fig. 6.1.2.1. The tube has a spirally wound tungsten filament, F, placed immediately behind a slot in the focusing cup, C, and a water-cooled target or anode, T, approximately 10 mm from the surface of C. The filament–focusing-cup assembly is at a negative voltage of between 30 and 50 kV, and the target is at ground potential. The electron beam strikes the target in a focal line,

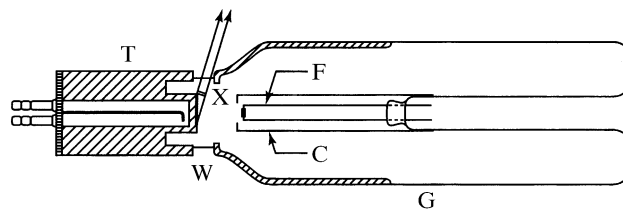


Fig. 6.1.2.1. Section through a sealed X-ray tube. G, glass envelope; F, filament leads (at negative high voltage); C, focusing cup; T, target (at ground potential); W, one of four beryllium windows. The electron beam forms a line on the target, which is viewed at a small take-off angle to form a foreshortened effective source X.

which acts as a line source of X-rays. There are usually two pairs of X-ray windows, W, through which the source is viewed at a small angle to the target surface, thus producing a foreshortened effective source, X, which is approximately square in one plane and a narrow line in the other. Focus dimensions on the target and maximum recommended power loading are shown for a number of standard inserts in Table 6.1.2.1. None of these are ideal for macromolecular crystallography. The assembly of a cathode, anode and windows – the tube insert – is inserted in a shock- and radiation-proof shield which is fixed to the table. Attached to the shield are X-ray shutters and filters, and sometimes brackets for bolting on X-ray cameras. A high-voltage connection is made to the tube by means of a flexible, shielded, shock-proof cable; nowadays, this high voltage is almost invariably full-wave rectified and smoothed DC.

##### 6.1.2.2. Rotating-anode X-ray tubes

The sealed tubes described above are convenient and require little maintenance, but their power dissipation, and thus their X-ray output, is limited. For macromolecular crystallography, the most commonly used tubes are continuously pumped, demountable tubes with water-cooled rotating targets [see the reviews by Yoshimatsu & Kozaki (1977) and Phillips (1985)]. At present, these tubes mostly employ ferro-fluidic vacuum shaft seals (Bailey, 1978), which have an operational life of several thousand hours before they need replacement. The need for a beam with a small cross fire calls for a focal spot preferably not larger than  $0.15 \times 0.15$  mm. This is usually achieved by focusing the electrons on the target to a line 0.15 mm wide and 1.5 mm long (in the direction parallel to the rotation axis of the target). The line is then viewed at an angle of  $5.7^\circ$  to give a 10:1 foreshortening. Foci down to this size can be produced on a target mounted close to an electron gun. For smaller focal spots, such as those of the microfocuss tube described below, it

Table 6.1.2.1. Standard X-ray tube inserts

Focus size on target (mm × mm)	Recommended power loading (kW)
8 × 0.15	0.8
8 × 0.4	1.5
10 × 1.0	2.0
12 × 2.0	2.7

## 6. RADIATION SOURCES AND OPTICS

is necessary to employ an electron lens (which may be magnetic or electrostatic) to produce on the target a demagnified image of the electron cross-over, which is close to the grid of the tube cathode.

The maximum power that can be dissipated in the target without damaging the surface has been discussed by Müller (1929, 1931), Oosterkamp (1948), and Ishimura *et al.* (1957). The later calculations are in adequate agreement with Müller's results, from which the power  $W$  for a copper target is given by

$$W = 26.4 f_1 (f_2 \nu)^{1/2}.$$

Here,  $W$  is in watts,  $f_1$  and  $f_2$  are the length and the width of the focal line in mm, and  $\nu$  is the linear speed of the target surface in  $\text{mm s}^{-1}$ ; it is assumed that the surface temperature of the target reaches  $600^\circ\text{C}$ , well below the melting point of copper ( $1083^\circ\text{C}$ ). Thus, for a focal spot  $1.5 \times 0.15$  mm and for an 89 mm-diameter target rotating at  $6000$  revolutions  $\text{min}^{-1}$  ( $\nu = 28\,000$   $\text{mm s}^{-1}$ ), Müller's formula gives a maximum permissible power loading of  $2.5$  kW or  $57$  mA at  $45$  kV. This agrees well with the experimentally determined loading limit.

Green & Cosslett (1968) have made extensive measurements of the efficiency of the production of characteristic radiation for a number of targets and for a range of electron accelerating voltages. Their results have been verified by many subsequent investigators. For a copper target, they found that the number of  $K\alpha$  photons emitted per unit solid angle per incident electron is given by

$$N/4\pi = 6.4 \times 10^{-5} [E/E_k - 1]^{1.63},$$

where  $E$  is the tube voltage in kV and  $E_k = 8.9$  keV is the  $K$  excitation voltage.

Accordingly, the number of  $K\alpha$  photons generated per second per steradian per mA of tube current is  $1.05 \times 10^{12}$  at  $25$  kV and  $4.84 \times 10^{12}$  at  $50$  kV.

Of the generated photons, only a fraction, usually denoted by  $f(\chi)$  (Green, 1963), emerges from the target as a result of X-ray absorption in the target.  $f(\chi)$  decreases with increasing tube voltage and with decreasing take-off angle. It has a value of about  $0.5$  for  $E = 50$  kV and for a take-off angle of  $5^\circ$ .

The X-ray beam is further attenuated by absorption in the tube window ( $\sim 80\%$  transmission), by the air path between the tube and the sample, and by any  $\beta$ -filters which may be used.

In a typical diffractometer or image-plate arrangement where no beam conditioning other than a  $\beta$ -filter is employed, the sample may be  $300$  mm from the tube focus and the limiting aperture at that point might have a diameter of  $0.3$  mm, so that the full-angle cross fire at the sample is  $1.0 \times 10^{-3}$  rad. The solid angle subtended by the limiting aperture at the source is  $7.9 \times 10^{-7}$  steradians. At  $50$  kV and  $60$  mA, the X-ray flux through the sample will be approximately  $4.5 \times 10^7$  photons  $\text{s}^{-1}$ . These figures are approximately confirmed by unpublished experimental measurements by Arndt & Mancina and by Faruqi & Leslie. It is interesting to note that the power in this photon flux is  $5.8 \times 10^{-8}$  W, which is a fraction of  $2 \times 10^{-11}$  of the power loading of the X-ray tube target.

Instead of simple aperture collimation, one of the types of focusing collimators described in Section 6.1.4.1 below may be used. They collect a somewhat larger solid angle of radiation from the target of a conventional X-ray source than does a simple collimator and some produce a higher intensity at the sample.

### 6.1.2.3. Microfocus X-ray tubes

Standard sealed X-ray tubes with a stationary target deliver a collimated intensity to the sample which is insufficient for most applications in macromolecular crystallography. These tubes have foreshortened foci between  $0.4$  and  $2$   $\text{mm}^2$  which do not lend themselves to efficient collimation by means of focusing mirrors or

monochromators without introducing a cross fire in the beam that is too large for our purposes.

The situation is different with microfocus tubes, which are discussed in Section 6.1.4.2. Here, a relatively large solid angle of collection can make up for the lower power dissipation which results from the small electron focus.

### 6.1.2.4. Synchrotron-radiation sources

Charged particles with energy  $E$  and mass  $m$  moving in a circular orbit of radius  $R$  at a constant speed  $v$  radiate a power,  $P$ , into a solid angle of  $4\pi$ , where

$$P = 88.47E^4 I / R,$$

where  $E$  is in GeV,  $I$  is the circulating electron or positron current in amperes and  $R$  is in metres. Thus, for example, in a bending-magnet beam line at the ESRF, Grenoble, France,  $R = 20$  m, and at  $5$  GeV and  $200$  mA,  $P = 554$  kW.

For relativistic electrons, the electromagnetic radiation is compressed into a fan-shaped beam tangential to the orbit, with a vertical opening angle  $\Psi \simeq mc^2/E$ , *i.e.*  $0.1$  mrad for  $E = 5$  GeV (Fig. 6.1.2.2). This fan rotates with the circulating electrons; if the ring is filled with  $n$  bunches of electrons, a stationary observer will see  $n$  flashes of radiation every  $2\pi R/c$  s, the duration of each flash being less than  $1$  ns.

The spectral distribution of synchrotron radiation extends from the infrared to the X-ray region; Schwinger (1949) gives the instantaneous power radiated by a monoenergetic electron in a circular motion per unit wavelength interval as a function of wavelength (Winick, 1980). An important parameter specifying the distribution is the critical wavelength,  $\lambda_c$ : half the total power radiated, but only  $\sim 9\%$  of the total number of photons, is at  $\lambda < \lambda_c$  (Fig. 6.1.2.6).  $\lambda_c$  (in Å) is given by

$$\lambda_c = 18.64 / (BE^2),$$

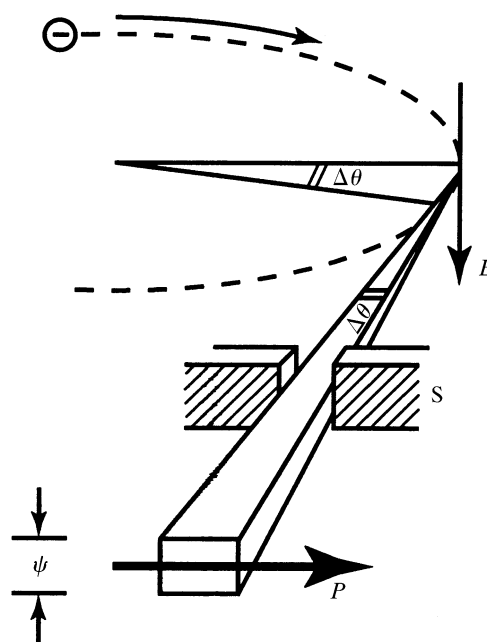


Fig. 6.1.2.2. Synchrotron radiation emitted by a relativistic electron travelling in a curved trajectory.  $B$  is the magnetic field perpendicular to the plane of the electron orbit;  $\psi$  is the natural opening angle in the vertical plane;  $P$  is the direction of polarization. The slit,  $S$ , defines the length of the arc of angle,  $\Delta\theta$ , from which the radiation is taken. From Buras & Tazzari (1984).

## 6.1. X-RAY SOURCES

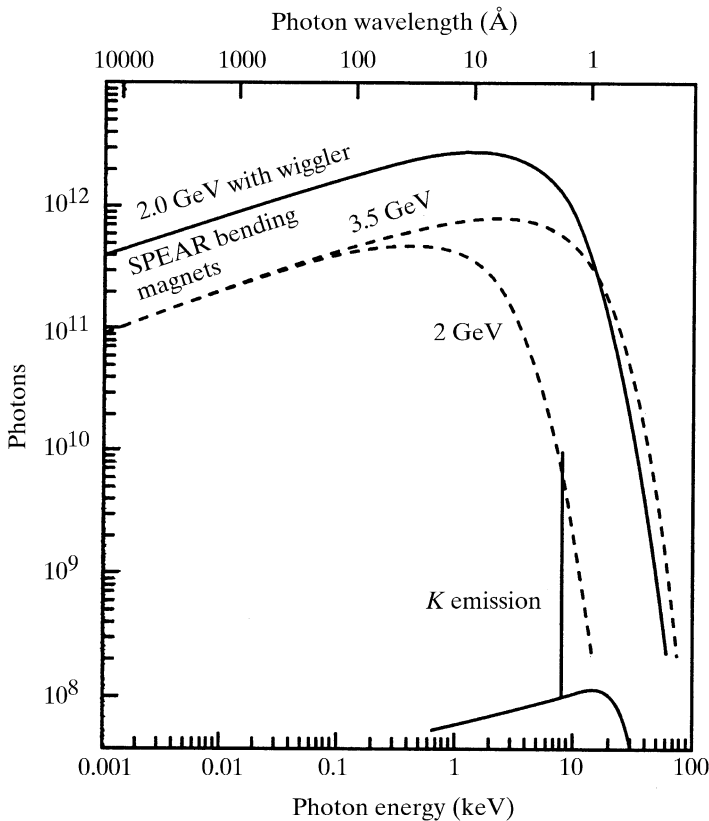


Fig. 6.1.2.3. Comparison of the spectra from the storage ring SPEAR in photons  $\text{s}^{-1} \text{mA}^{-1} \text{mrad}^{-1}$  per 1% band pass (1978 performance) and a rotating-anode X-ray generator, showing the Cu *K* emission line and the *Bremsstrahlung*. Reproduced with permission from Nagel (1980). Copyright (1980) New York Academy of Sciences.

where  $B (= 3.34E/R)$  is the magnetic bending field in T,  $E$  is in GeV and  $R$  is in metres.

The orbit of the particle can be maintained only if the energy lost, in the form of electromagnetic radiation, is constantly replenished. In an electron synchrotron or in a storage ring, the circulating particles are electrons or positrons maintained in a closed orbit by a magnetic field; their energy is supplied or restored by means of an oscillating radiofrequency (RF) electric field at one or more places in the orbit. In a synchrotron designed for nuclear-physics experiments, the circulating particles are injected from a linear accelerator, accelerated up to full energy by the RF field, and then deflected onto a target with a cycle frequency of about 50 Hz. The synchrotron radiation is thus produced in the form of pulses of this

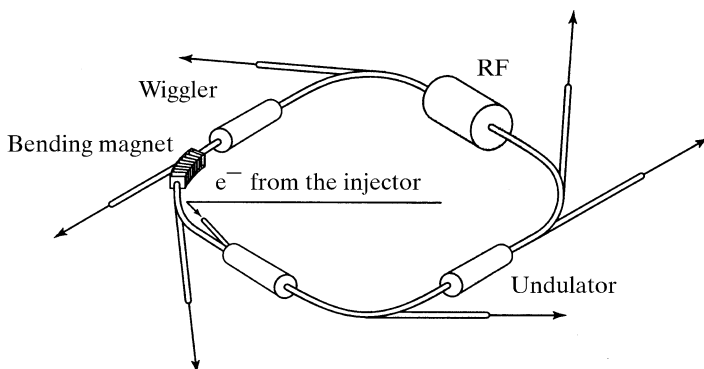


Fig. 6.1.2.4. Main components of a dedicated electron storage-ring synchrotron-radiation source. For clarity, only one bending magnet is shown. From Buras & Tazzari (1984).



Fig. 6.1.2.5. Electron trajectory within a multipole wiggler or undulator.  $\lambda_0$  is the spatial period,  $\alpha$  is the maximum deflection angle and  $\theta$  is the observation angle. From Buras & Tazzari (1984).

frequency. A storage ring, on the other hand, is filled with electrons or positrons, and after acceleration the particle energy is maintained by the RF field; ideally, the current circulates for many hours and decays only as a result of collisions with remaining gas molecules. At present, only storage rings are used as sources of synchrotron radiation, and many of these are dedicated entirely to the production of radiation: they are not used at all, or are used only for limited periods, for nuclear-physics collision experiments.

Synchrotron radiation is highly polarized. In an ideal ring, where all electrons are parallel to one another in a central orbit, the radiation in the orbital plane is linearly polarized with the electric vector lying in this plane. Outside the plane, the radiation is elliptically polarized.

In practice, the electron path in a storage ring is not a circle. The 'ring' consists of an alternation of straight sections and bending magnets. Beam lines are installed at the bending magnets and at the insertion devices.

These insertion devices with a zero magnetic field integral, *i.e.* wigglers and undulators, may be inserted in the straight sections (Fig. 6.1.2.4). A wiggler consists of one or more dipole magnets with alternating magnetic field directions aligned transverse to the orbit. The critical wavelength can thus be shifted towards shorter values because the bending radius can be decreased over a short section, especially when superconducting magnets are used. Such a device is called a wavelength shifter. If it has  $N$  dipoles, the radiation from the different poles is added to give an  $N$ -fold increase in intensity. Wigglers can be horizontal or vertical. In a wiggler, the maximum divergence,  $2\alpha$ , of the electron beam is much larger than  $\psi$ , the vertical aperture of the radiation cone in the spectral region of interest (Fig. 6.1.2.2). If  $2\alpha \ll \psi$ , and if, in addition, the magnet poles of a multipole device have a short period, then the device becomes an undulator; interference takes place between the radiation of wavelength  $\lambda_0$  emitted at two points  $\lambda_0$  apart on the electron trajectory (Fig. 6.1.2.5). The spectrum at an angle  $\theta$  to the axis observed through a pinhole consists of a single spectral line and its harmonics with wavelengths

$$\lambda_i = i^{-1} \lambda_0 [(E/mc^2)^{-2} + \alpha^2/2 + \theta^2]/2$$

(Hofmann, 1978). Typically, the bandwidth of the lines,  $\delta\lambda/\lambda$ , is  $\sim 0.01$  to  $0.1$ , and the photon flux per unit bandwidth from the undulator is many orders of magnitude greater than that from a bending magnet. Undulators at the ESRF have a fundamental wavelength of less than  $1 \text{ \AA}$ .

The spectra for a bending magnet and a wiggler are compared with that from a copper-target rotating-anode tube in Fig. 6.1.2.3.

### 6.1.3. Properties of the X-ray beam

We must now consider the properties of the X-ray beam necessary for the gathering of intensity data from single crystals of biological macromolecules. The properties of the beam with which we are concerned are:

- the size of the beam appropriate for the sample dimensions;
- the X-ray wavelength and its spectral purity;
- the intensity in photons  $\text{s}^{-1}$ ;